Progress In Electromagnetics Research C, Vol. 66, 87–95, 2016

Small-Size Coupled-Fed Two Opposite-Direction Spiral Branches for Handset Antenna

Ping Wang[1, 2, *] and Can Cui[1]

Abstract—A compact coupled-fed handset antenna with multi-frequency band operation is proposed in this paper. It occupies a no-ground space of only $26 \times 14\,\text{mm}^2$, and two wideband operations can be achieved by the coupled-fed two opposite-direction spiral branches. The low frequency bands of LTE700 operation are achieved by two spiral branches' 0.25-wavelength monopole modes, which generate a dual-resonance mode at 740 and 780 MHz. At around high frequency ranges, a 0.25-wavelength monopole mode of a T-shaped monopole is generated at 1.75 GHz, and combined with two 0.75-wavelength high-order monopole modes of the left and right side spiral branches to cover the DCS1800/PCS1900/UMTS2100/LTE2300/2500 bands. In addition, the proposed antenna is easily printed on the dielectric surface of a low cost FR4 substrate, which makes it suitable for practical mobile applications. The proposed antenna is successfully simulated, fabricated, and measured to validate the design.

1. INTRODUCTION

In the last decades, wireless communication system has grown rapidly with a lot of developments. Its technology performance has evolved from 1G to digital 2G, through 3G, to 4G, and the future 5G system, gradually. This also induces the market demands for wireless mobile terminal such as mobile phones. As a key component in modern mobile terminal system, antenna plays an important role of effectively receiving and sending electromagnetic wave signals which can not only improve the communication quality, but also influence the power dissipation radiation and external structure of mobile phones. Thus, studying and designing high-performance antenna has become a subject of interest for a long time.

The LONG Term Evolution (LTE) system with LTE700 (698–787 MHz), LTE2300 (2300–2400 MHz), and LTE2500 (2500–2690 MHz) operating bands [1] has attracted great attention for the use in 4G wireless wide area network (WWAN) systems to incorporate the LTE system with 2G and 3G system mobile devices. This is done to achieve higher data transmission and improve communication quality. As such, the handset antennas should be with compact sizes and wide operating bands to ensure the ability to embed into the limited space and operation in 2G/3G/4G systems. For handset antenna designing, the biggest challenge lies in the covering of the low frequency band, especially in LTE700 band. To realize the characteristic, a monopole structure may be an interesting candidate owing to its simple working mechanism, flexible adjustment modes, high integration with active devices, etc. Thus, several printed monopole coupled configurations for mobile phone have been proposed [2–9]. In [2], an on-board coupled-fed monopole antenna was presented, which consists of a feeding strip and a distributed inductive shorted strip. The antenna achieves a seven-band WWAN/LTE operation covering

Received 5 May 2016, Accepted 10 July 2016, Scheduled 19 July 2016

* Corresponding author: Ping Wang (wp@cqupt.edu.cn).

[1] School of Communication and Information Engineering, Chongqing University of Posts and Telecommunications, Chongqing 400065, China. [2] Collaborative Innovation Center for Information Communication Technology, and Electronic Information and Networking Research Institute, Chongqing University of Posts and Telecommunications, Chongqing 400065, China.

824–960/1710–2690 MHz frequency ranges and occupies a size of $15 \times 29\,\text{mm}^2$, but LTE700 band is not covered because it is difficult to obtain LTE700 band in an electrical small antenna. Similarly, several planar printed coupled-fed monopole antennas with multi-band operations are presented for ultra-slim mobile handset applications in [3–7] and use monopole coupled fed way to realize broad band operation, but these antennas have a large no-ground area of generally larger than $15 \times 50\,\text{mm}^2$. A 3-dimension monopole coupled-fed structure was also proposed for covering $698 \sim 960$ MHz and $1710 \sim 2690$ MHz bands [8], but the antenna has a large no-ground space of $24 \times 60\,\text{mm}^2$ and three-dimensional structures, which may not be appropriate when integration and slimmer design is concerned. In [9], a planar printed coupled-fed loop antenna for designing multiple-input multiple-output (MIMO) handset applications is proposed to cover $0.747 \sim 0.787$ GHz and $1.7 \sim 3.04$ GHz, but the antenna occupies a large no-ground area of $22.5 \times 24\,\text{mm}^2$. Recently, the magneto-dielectric (MD) material was also used in designing a handset antenna to reduce the antenna size and improve the bandwidth of smartphone [10]. Though the antenna operates in about 745–973 and 1536–2825 MHz, the no-ground space size is $15 \times 35\,\text{mm}_2$, and the antenna has three-dimensional structures. Thus, it can be seen that to realize small no-ground space and wideband operation for such an antenna, there is still a long way to go.

In this paper, a planar printed multi-band monopole antenna for a mobile phone is proposed, which is easy to fabricate on a thin FR4 substrate of $120 \times 60\,\text{mm}^2$ and is able to provide two wide operating bands. Dual resonances in the lower band are generated by the 0.25-wavelength monopole modes of two spiral branches, while in the upper band a wide bandwidth of more than 1000 MHz (1665 MHz–2715 MHz) is achieved by combining the high modes of spiral branches and 0.25-wavelength monopole mode of the T-shaped monopole. The antenna is studied using the package ANSYS high-frequency structure simulator (HFSS). An experimental prototype for the proposed antenna is fabricated and measured to verify the simulation and findings.

2. ANTENNA CONFIGURATION

Figure 1 illustrates the geometry and detailed parameters of the proposed antenna, whereas Figure 2 illustrates the enlargement dimensions of the metal pattern in the antenna area. The proposed antenna consists of three copper layers which are a T-shaped feeding strip and two opposite-direction spiral branches with different lengths. The two spiral branches are located in the exterior of two dielectric substrates, and two dielectric substrates sandwich the T-shaped feeding monopole. This layout contains two spiral branches to generate 0.25-wavelength monopole mode aiming to form dual resonances in low band and combines 0.75-wavelength high-order modes of the spiral branches with 0.25-wavelength monopole mode of the T-shaped monopole strip to cover the upper

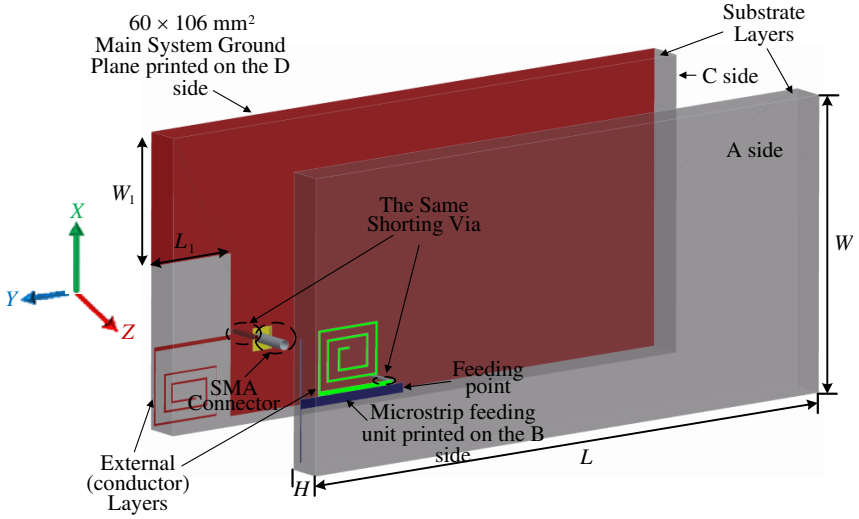

Figure 1. Configuration of the proposed antenna.

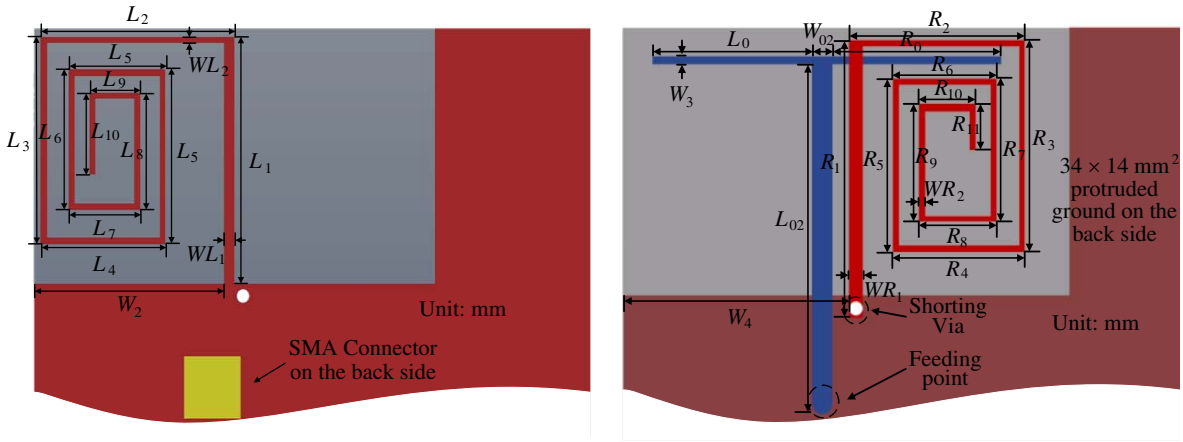

Figure 2. Detailed dimensions of the metal pattern in the antenna area.

Table 1. The detail parameters of proposed antenna.

Detail parameters	Size (mm)	Detail parameters	Size (mm)	Detail parameters	Size (mm)
L	120	H	1	W	60
W_{01}	34	L_{01}	14	L_1	13.8
L_2	12.8	L_3	12.1	L_4	7.5
L_5	10.75	L_6	6.15	L_7	9.4
L_8	4.8	L_9	8	L_{10}	3.4
L_{11}	7	WL_1	0.8	WL_2	0.4
W_2	12.2	R_1	15.8	R_2	10
R_3	12.1	R_4	8	R_5	10.3
R_6	6.6	R_7	9	R_8	5.3
R_9	7.6	R_{10}	3.9	R_{11}	4
W_{02}	1.5	W_3	0.5	W_4	13.1
L_0	8.5	R_0	8.5	L_{02}	21.05
WR_1	0.8	WR_2	0.4		

band. Finally, through appropriately changing the length and width of drive strip, two operating bands are formed to satisfy working frequency band of various wireless communication systems such as LTE700/DCS1800/PCS1900/UMTS2100/LTE2300/2500 and WLAN bands, etc. It should be mentioned that the location parameters of the T-shaped monopole strip may be adjusted carefully for producing a good impedance match.

As shown in Figure 1, two FR4 substrate boards (dielectric constant = 4.4, loss tangent = 0.02) with a thickness of 0.5 mm has been employed as the system circuit board of mobile handset, and the planar size is about $60 \times 120\,\text{mm}^2$. A main system ground plane with a size about $60 \times 106\,\text{mm}^2$ is printed on the back layer ("D" side) of the substrate, and a protruded ground plane with a size of $14 \times 34\,\text{mm}^2$ on the top right side is integrated with the system ground plane, leaving a non-grounded area of $14 \times 26\,\text{mm}^2$ at the top left side of the substrate to accommodate the proposed antenna. A right-hand spiral branch on the surface of a dielectric substrate is integrated directly to the top side of the system ground plane, yet another left-hand spiral branch on "A" side is connected to the system ground plane by using a shorting via. The T-shaped feeding metal strip on "B" side is connected to the inner conductor of a $50\,\Omega$ SMA connector through via-hole for testing the antenna. The external layer of the SMA connector is soldered to the system ground plane. The optimized parameters are illustrated in Table 1.

3. SIMULATED AND MEASURED RESULTS

To better understand the effect of left- or right-hand spiral monopole on reflection coefficient, only a spiral monopole is integrated with the system ground plane in simulation software, while other parameters are kept unchanged, as shown in Figure 3.

The simulated S_{11} results are shown in Figure 4, from which it is seen that right-hand spiral monopole (branch 1) generates a 0.25-wavelength monopole resonant mode at low-frequency band on the left side of 760 MHz, and its high-frequency resonance scope is between 1740 and 2370 MHz. However, the left-hand spiral monopole (branch 2) produces another 0.25-wavelength monopole resonant mode on the right side of 760 MHz, and the upper band is about 1600–2600 MHz. By combining with the fundamental mode of the two 0.25-wavelength monopole modes, a dual-resonance bandwidth is formed to cover LTE700 operation bands. From Figure 4, we can see that two coupled-fed branches produce two resonance modes around 760 MHz, respectively. It means that the two resonance modes can be combined to form a dual-resonance when the two branches exist simultaneously. But bandwidth of the two low-frequency bands is not ideal to cover the whole LTE700. When two branches of an antenna are introduced, low frequency bandwidth is enlarged, which is less than −6 dB. Similarly, bandwidth in the high frequency is also enlarged, and a bandwidth of 1665–2715 MHz assuming the −6 dB reflection coefficient as a reference is obtained.

Figure 5 shows simulated surface current distribution diagram of the designed antenna undertaken in HFSS. Double-helix coupling branch knot mostly affects the low-frequency resonance of the antenna. When the antenna works in 740 MHz, current is mainly distributed in the left helix coupling unit, which

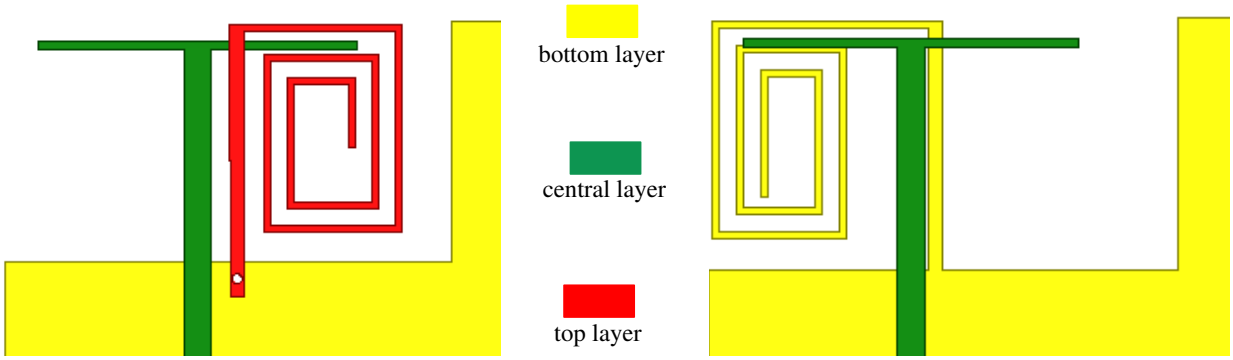

Figure 3. Different branch structures. (a) Right-hand spiral monopole, (b) left-hand spiral monopole.

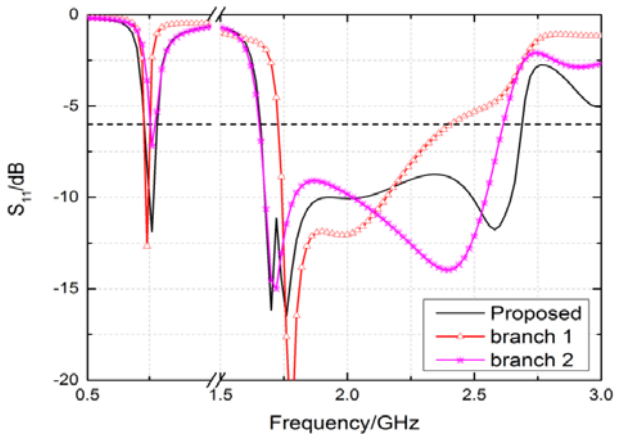

Figure 4. Simulated reflection coefficient for the different branch structures.

is matched with the low-frequency central resonance frequency of branch knot 2 in Figure 4; when the antenna works in 780 MHz, current is mainly distributed in the right helix coupling unit, which is also matched with the low-frequency central resonance frequency of branch knot 1 in Figure 4; when the antenna works in 2.2 GHz, current is mainly distributed in the left helix coupling unit and driver unit, which shows that the surface current of the driver unit in 2.5 GHz is more active than the current in 2.2 GHz. Long current path should be resonant with the corresponding low-frequency resonance, while the short one should be resonant with the high-frequency resonance. It is consistent with the analysis of simulated results of each branch knot in Figure 4. Under the effect of the driver unit, resonance of the antenna in 2.5 GHz is stronger than the high-frequency resonance of 2.2 GHz.

Figure 6 shows the influence of coupling branch L_{11} and R_{11} parameters on the antenna reflection coefficient. We can see from Figure 6 that the decrease in length of coupling branch knot L_{11} and R_{11} of the antenna has extremely small influence on the antenna's S_{11}. Likewise, we can see from the simulated surface current distribution of the antenna in Figure 5 that the induced current on L_{11} and R_{11} is not active under the frequencies of 740 MHz and 780 MHz. The decrease in length of L_{11} and R_{11} causes the high-frequency bandwidth of the antenna to decrease, while the performance of the antenna decreases gradually. When $L_{11} = 1$ mm and $R_{11} = 1$ mm, high-frequency operating frequency of the antenna is

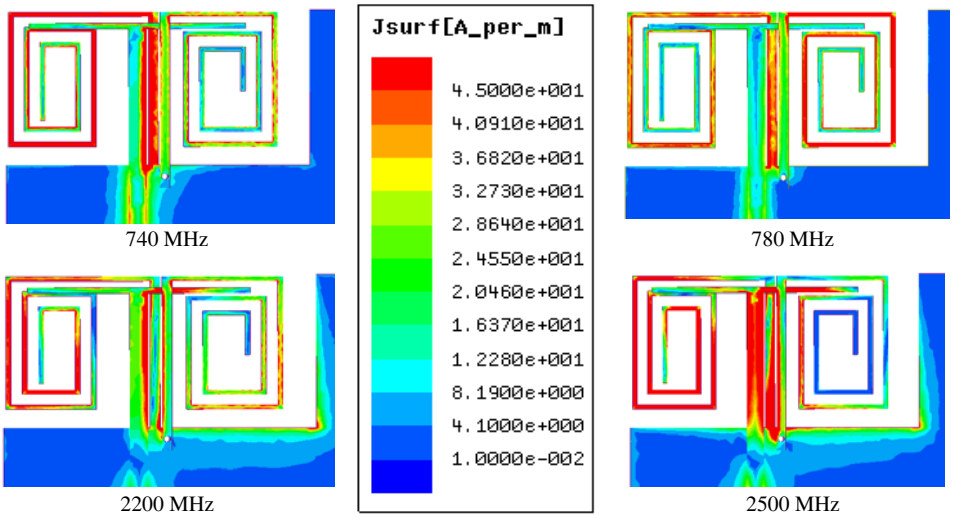

Figure 5. Simulated surface current distributions on the antennas and system ground plane.

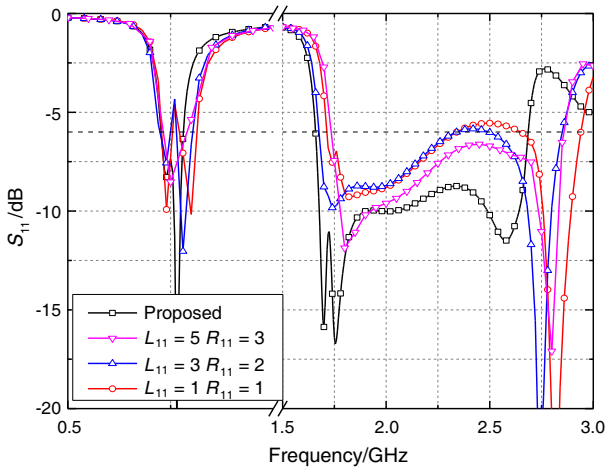

Figure 6. Simulated reflection coefficient for the different length of L_{11} and R_{11}.

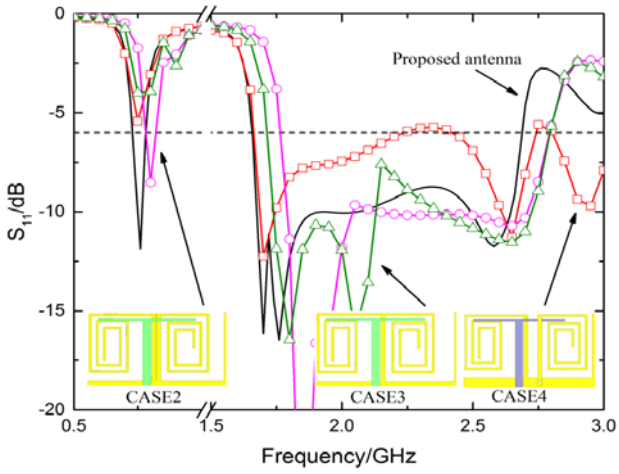

Figure 7. Simulated reflection coefficient for the similar structure.

influenced greatly. Thus, coupling branch knots L_{11} and R_{11} in appropriate lengths are necessary.

To prove the importance of multilayer structure for the designed antenna, simulated S_{11} results of three antennas with a similar structure are presented in Figure 7. Length and width parameters of coupling and driver units for the helix structure of the three antennas are similar to that of the designed antenna. CASE2 is located on the single-layer FR4 dielectric-slab with the thickness of 0.5 mm, and the driver unit is located at the front side of the dielectric-slab; two coupling branch knots of the helix structure are located at the other side of the dielectric-slab; at the same time, their first bending sections tightly rely on each other. CASE3 structure is also located on the single-layer FR4 dielectric-slab with thickness of 0.5 mm. The only difference between this antenna and antenna 2 is that the coupling branch knot of the helix structure adopts the parasitic method of left helix coupling unit driving the right helix branch knot. CASE4 structure is similar to the structure of the designed antenna, which is printed on each surface of a double-layer dielectric-slab with a thickness of 0.5 mm. The difference is the gap distance between the two coupling branches of the x-axis dimension of CASE4 while others are kept unchanged.

From Figure 7, we can see that high-frequency and low-frequency resonances are shifted right compared with that of the designed antenna. The scope of high-frequency resonance of CASE2 is shifted right from 1680 MHz–2680 MHz of the designed antenna to 1750 MHz–2760 MHz, while low-frequency resonance is shifted right from 750 MHz to around 800 MHz with the narrowing bandwidth of low-frequency resonance and lower performance; the scope of high-frequency resonance of CASE3 is shifted right to 1720 MHz–2760 MHz, but low-frequency resonance cannot reach the design requirements of the antenna for phone terminal; high-frequency and low-frequency resonances of CASE4 fail to meet the performance index.

4. MEASUREMENT RESULTS

According to the theory, size parameters of the antenna are simulated and optimized to process real antenna object with feed hole, as shown in Figure 8. In the real processing process, a printed circuit board is adopted to print the structure of the antenna in the dielectric surface of two FR4 dielectric boards, and then the inner core of a 50 Ω SMA connector passing through a dielectrics lab is connected with the T-shaped driver circuit on the top surface of bottom dielectric board, while external conductor is welded with the ground plane directly. Finally, the top surface of bottom dielectric board is glued together with the bottom surface of the top dielectric board by using strong glue, and the right-hand spiral monopole is connected to the main ground plane by using fine copper wire through shorting via to form the proposed handset antenna.

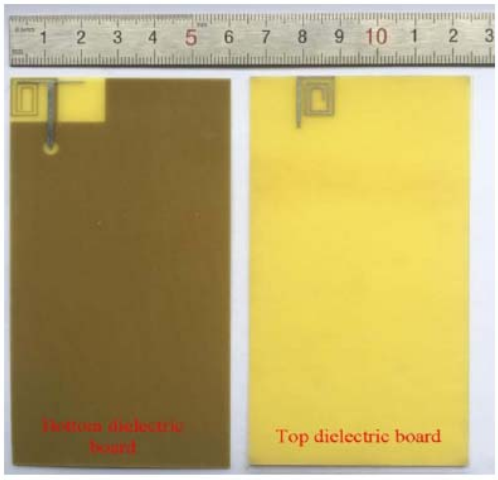

Figure 8. The prototype of the proposed antenna.

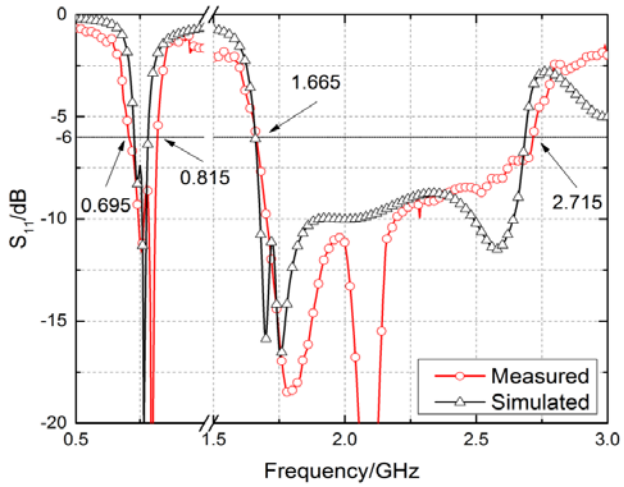

Figure 9. Simulated and measured S_{11} of the proposed antenna.

In testing, feed on the coaxial line of SMA connector with the characteristic impedance of 50 Ω is adopted to connect the feed hole of the real antenna object. Testing result is obtained from the vector network analyzer and antenna testing system and shown in Figure 9. It can be observed that the testing value is relatively identical to the simulated value. Deviation comes from: (1) Double-layer dielectrics lab of real antenna object adopts glue, of which the influence of electromagnetic radiation is not considered; (2) Own errors of testing instruments; (3) Errors in the testing process;

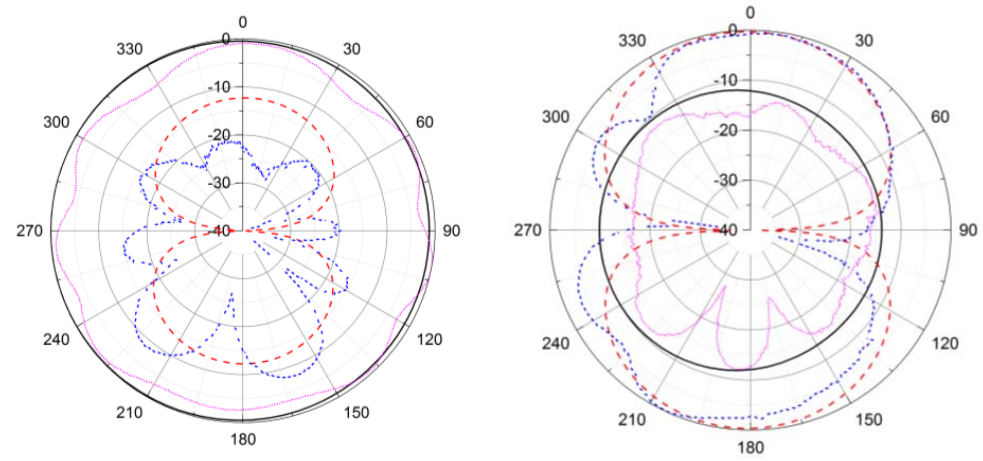

(a)

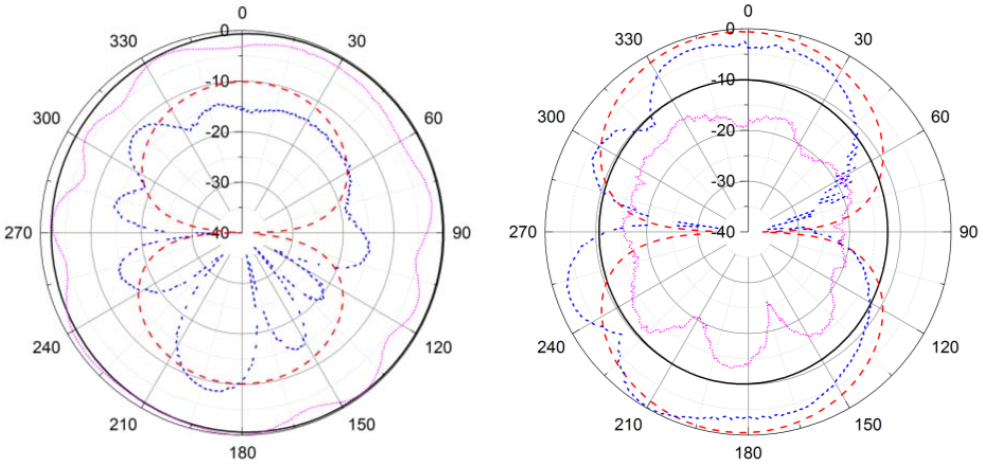

(b)

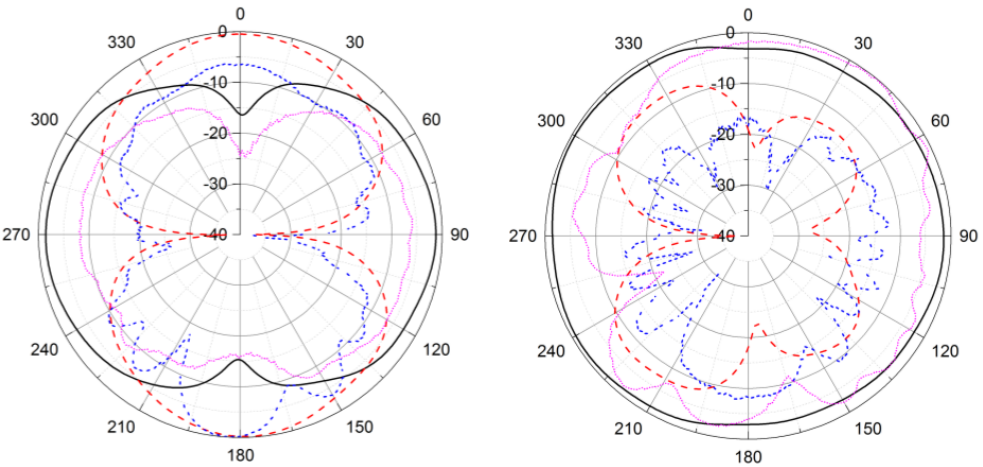

(c)

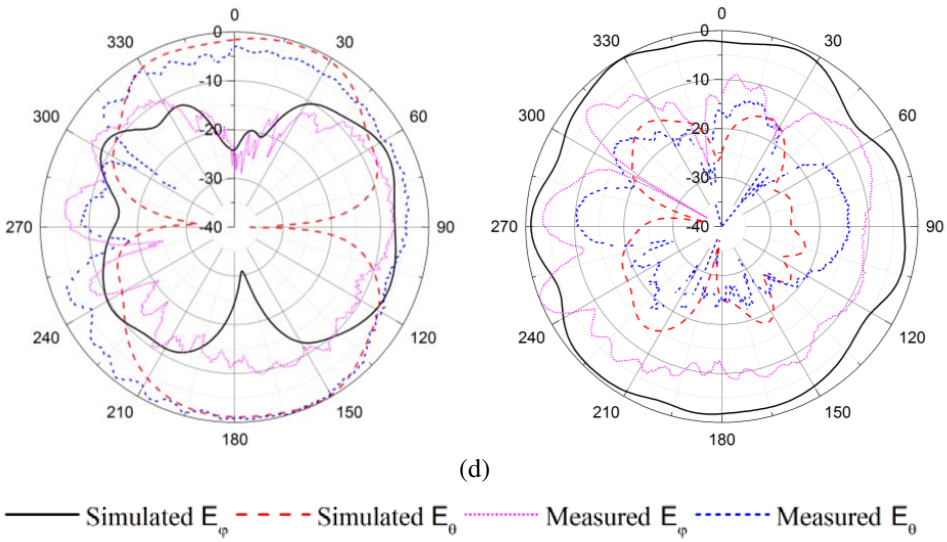

Figure 10. Simulated and measured normalized radiation patterns of the proposed antenna at different frequencies. (a) 780 MHz, (b) 920 MHz, (c) 2030 MHz, (d) 2600 MHz.

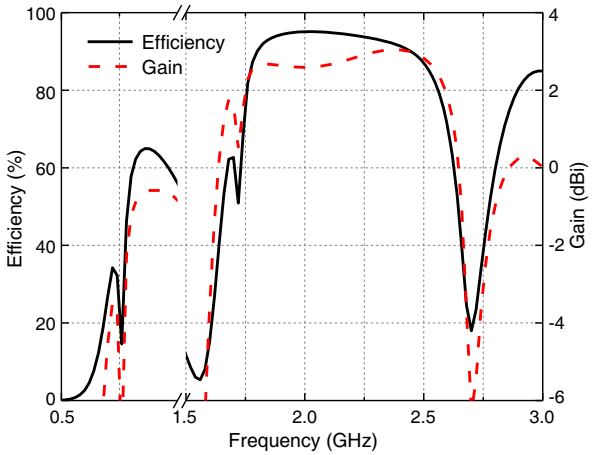

Figure 11. Realized gain and efficiency of the proposed antenna.

(4) Processing error of real antenna object. The testing result shows that the antenna has a good feature in back loss of the antenna under the frequency band of 695 MHz–815 MHz and 1665 MHz–2715 MHz, which can cover multiple work frequencies of important wireless communication systems, such as LTE700/DCS1800/PCS1900/UMTS2100/LTE2300/2500 and WLAN bands.

Figure 10 shows the simulated and measured radiation patterns of E and H planes in free spaces in the frequencies of 780 MHz, 920 MHz, 2030 MHz and 2600 MHz. It can be found from these diagrams that the antenna comes up with small portions of distortion in certain radioactive directions. Deviation of simulation and testing obtained from analysis might be from zero return of testing angle during test. Thus, a shift is generated in the directional angle of antenna pattern. Also, as it is the test for miniaturized mobile terminal antenna, it is hard to effectively control the current influence of feed cable, which affects the radiation pattern. However, in general, simulated and tested radiation patterns are similar to each other as a whole with the horizontally all-round radiation. With certain universality, the simulated antenna can be applied into various communication systems.

Figure 11 shows the gain and efficiency of the proposed antenna. The gains are between -3.5 to -2.2 dBi and 0.43 to 3 dBi at low and upper frequency bands, respectively. The efficiencies are between 27% and 46% and between 51% and 90% at the low and upper frequency bands, respectively. The radiation efficiency is acceptable and meets requirement for the practical WWAN/LTE mobile handset.

5. CONCLUSION

Based on coupled-fed mechanism, this paper presents a small-size planar printed mobile phone antenna with multi-band operations. The proposed antenna is composed of a T-shaped driving unit and two spiral branch units. The branch units produce two resonances at low frequencies, respectively, controlling the low frequency operating bandwidth, and the drive unit mainly controls the high frequency operating bandwidth. According to the calculation, simulation and optimization of antenna size parameters, the antenna was actually produced and tested. The result shows that the proposed antenna can generate multiple resonant modes at lower and upper bands for covering LTE700/DCS1800/PCS1900/UMTS2100/LTE2300/2500 and WLAN bands, and keeps a small no-ground space of only $26 \times 14\,\text{mm}^2$. The measured results are basically consistent with the software simulation ones to achieve the design requirements, which indicates that the proposed antenna is promising for planar smartphone applications.

ACKNOWLEDGMENT

This work was supported by the Mainland-Hong Kong-Macau-Taiwan science and technology cooperation projects (2015DFT10170), the National High Technology Research and Development Program of China (863 Program) under Grant No. 2014AA01A705, and Doctoral fund of Chongqing University of Posts and Telecommunications (A2015-08).

REFERENCES

1. The 3rd Generation Partnership Project, "LTE advanced," 2011, [Online], available: http://www.3-gpp.org/LTE-Advanced.
2. Ban, Y. L., C. L. Liu, J. L. W. Li, and R. Li, "Small-size wideband monopole with distributed inductive strip for seven-band WWAN/LTE mobile phone," *IEEE Antennas Wireless Propag. Lett.*, Vol. 12, 7–10, 2013.
3. Ku, C.-H., H.-W. Liu, and Y.-X. Ding, "Design of planar coupled-fed monopole antenna for eight-band LTE/WWAN mobile handset application," *Progress In Electromagnetics Research C*, Vol. 33, 185–198, 2012.
4. Bharti, P. K., G. K. Pandey, H. S. Singh, and M. K. Meshram, "A compact multiband planar monopole antenna for slim mobile handset applications," *Progress In Electromagnetics Research B*, Vol. 61, 31–42, 2014.
5. Huang, H.-F. and W. Zhao, "A small size three-band multi-functional antenna for LTE/GSM/UMTS/WIMAX handsets," *Progress In Electromagnetics Research Letters*, Vol. 49, 105–110, 2014.
6. Bharti, P. K., H. S. Singh, G. K. Pandey, and M. K. Meshram, "Thin profile wideband printed monopole antenna for slim mobile handsets application," *Progress In Electromagnetics Research C*, Vol. 57, 149–158, 2015.
7. Huang, H.-F. and W. Zhao, "Small-size 11-band LTE/WWAN/WLAN planar handset antenna," *Progress In Electromagnetics Research Letters*, Vol. 54, 39–45, 2015.
8. Dong, J., Y.-C. Jiao, Z.-B. Weng, Q. Qiu, and Y. Chen, "A coupled-fed antenna for 4G mobile handset," *Progress In Electromagnetics Research*, Vol. 141, 727–737, 2013.
9. Singh, H. S., G. K. Pandey, P. K. Bharti, and M. K. Meshram, "Compact printed diversity antenna for LTE700/GSM1700/1800/UMTS/Wi-Fi/Bluetooth/LTE2300/2500 applications for slim mobile handsets," *Progress In Electromagnetics Research C*, Vol. 56, 83–91, 2015.
10. Park, B. Y., M. H. Jeong, and S. O. Park, "A magneto-dielectric handset antenna for LTE/WWAN/GPS applications," *IEEE Antennas Wireless Propag. Lett.*, Vol. 13, 1482–1485, 2014.